200400564A

厚生労働科学研究研究費補助金

感覚器障害研究事業

強度近視における血管新生黄斑症の包括的治療法の確立に関する研究

平成16年度　総括研究報告書

主任研究者　大野　京子

平成17（2005）年　3月

目　次

I.　総括研究報告 ---------- 1

強度近視における血管新生黄斑症の包括的治療法の確立に関する研究

II.　研究成果の刊行に関する一覧表 ---------- 2

III.　研究成果の刊行物・別刷 ---------- 3

厚生労働科学研究費補助金（感覚器障害研究事業）
（総括）分担研究報告書

強度近視における血管新生黄斑症の包括的治療法の確立に関する研究

主任研究者　大野　京子
東京医科歯科大学大学院医歯学総合研究科講師

研究要旨；強度近視眼において血管新生が生じるメカニズムをヒト網膜色素上皮細胞に機械的伸展を負荷して基礎的に解明するとともに，脈絡膜新生血管を有する強度近視患者に光線力学療法もしくは triamcinolone acetonide の後部テノン嚢下投与を施行し治療効果を明らかにした。

分担研究者　森田育男，東京医科歯科大学大学院医歯学総合研究科教授，望月　學，東京医科歯科大学大学院医歯学総合研究科教授

A. 研究目的

わが国は世界有数の近視国であり，強度近視による視覚障害は常に失明原因の上位を占める。中でも黄斑部に生じる脈絡膜新生血管，いわゆる近視性血管新生黄斑症は強度近視患者の失明原因として注目されているが，本症に対する有効な治療は確立されていない。そこで本研究では，本症における新生血管発生機序を解明するとともに，すでに発生した新生血管に対しては，光線力学療法(PDT)とステロイド剤である triamcinolone acetonide (TA)をわが国ではじめて本症患者に臨床応用し，その短期的な効果を解明することを目的とする。

B. 研究方法

基礎的検討としては，強度近視の病態である眼軸の延長を模して，ヒト網膜色素上皮細胞(RPE)に機械的伸展を負荷して培養した際に生じる血管新生関連因子の遺伝子発現変化を検討するとともに，種々の薬剤により上記の発現変化が抑制できるか調べる。同時に臨床的検討として，文書による同意が得られた本症患者に対し，PDT もしくは TA の眼球後部テノン嚢下投与を施行し，短期的治療効果を明らかにする。

（倫理面への配慮）

PDT および TA 投与に対しては学内倫理委員会の承認を取得済みである。PDT および TA の臨床応用についてはヘルシンキ宣言を遵守し，患者から文書によるインフォームド・コンセントを得て行う。

C. 研究結果

機械的刺激負荷時のヒト RPE においては，血管新生抑制因子である色素上皮由来因子 PEDF の発現は変化しなかったが，血管内皮増殖因子 VEGF の著明な発現上昇がみられた。培地中に dexamethasone, indomethacin を添加すると VEGF の発現上昇が抑制された。

本症患者に対し TA のテノン嚢下投与を施行すると，新生血管の早期退縮が促進され，特に傍中心窩新生血管の症例では治療 3，6 ヵ月後に有意な視力改善が得られた。また PDT 治療により，全例で治療後早期に新生血管の閉塞がみられ出血吸収に伴い視力が改善した。

D. 考察

以上から眼軸の延長に伴う機械的刺激による RPE 細胞由来の血管新生関連因子の発現変化が本症における血管新生に関与する可能性が示唆された。また抗炎症薬の投与によりこれらの発現変化が抑制されたことから，本症に対するこれら薬剤の有用性が示唆された。また PDT および TA は本症患者の新生血管閉塞に有効であり短期予後の改善が認められた。

E. 結論

本症における血管新生の発生機序として，機械的刺激の負荷による RPE 由来の血管新生関連因子の発現変化が重要であり，これらに対してはステロイド剤もしくは NSAIDs を用いた治療が有効である可能性がある。さらに，すでに発生した新生血管に対しては PDT 及び TA が新生血管閉塞に有効であり本症の短期予後を改善することができる。

F. 健康危険情報

なし

G. 研究発表

1. 論文発表

Hayashi K, Ohno-Matsui K, Mochizuki M, et al. Characteristics of patients with a favorable natural course of myopic choroidal neovascularization. Graefes Arch Clin Exp Ophthalmol 243:13-19, 2005

Ohno-Matsui K, Ichinose S, Nakahama K, Yoshida T, Kojima A, Mochizuki M, Morita I. The effects of amniotic membrane on retinal pigment epithelial cell differentiation. Mol Vis 11:1-10, 2005

2. 学会発表

Yoshida T, Ohno-Matsui K, Kojima A, Morita I, Mochizuki M. Amyloid-beta regulates gene expression of angiogenesis-related factors in human retinal pigment epithelial cells. ARVO meeting 2004

吉田武史・大野京子・森田育男・望月　學，他．ヒト網膜色素上皮細胞における amyloid β 負荷時の血管新生関連因子の遺伝子発現変化．第 108 回日本眼科学会総会 2004

小島有里子・大野京子・森田育男・望月　學，他．近視性脈絡膜新生血管に対するトリアムシノロンの有用性．第 43 回日本網膜硝子体学会 2004

飛田秀明・大野京子・林　憲吾・吉田武史・島田典明・小島有里子・二神　創・所　敬・望月　學．近視性脈絡膜新生血管に対する光線力学療法の短期経過．2005 年東京医科歯科大学眼科同門会集談会

H. 知的所有権の出願・取得状況

なし

研究成果の刊行に関する一覧表

発表者氏名	論文タイトル名	発表誌名	巻号	ページ	出版年
Hayashi K, Ohno-Matsui K, et al.	Characteristics of patients with favorable natural course of myopic choroidal neovascularization.	Graefes Arch Clin Exp Ophthalmol	243	13-19	2005
Ohno-Matsui K, Ichinose S, et al.	The effect of amniotic membrane on retinal pigment epithelial cell differentiation.	Mol Vis	11	1-10	2005
Shimada N, Ohno-Matsui K, et al.	Characteristics of peripapillary detachment in pathologic myopia.	Arch Ophthalmol	in press		
Kobayashi K, Ohno-Matsui K, et al.	Fundus characteristics of high myopia in children	Jpn J Ophthalmol	in press		
Hayashi K, Ohno-Matsui K, et al.	RPE atrophy secondary to dilated choroidal artery in the macula in a highly myopic patient.	Jpn J Ophthalmol	in press		

Graefe's Arch Clin Exp Ophthalmol
(2005) 243:13–19

CLINICAL INVESTIGATION

DOI 10.1007/s00417-004-0960-5

Kengo Hayashi
Kyoko Ohno-Matsui
Takeshi Yoshida
Kanako Kobayashi
Ariko Kojima
Noriaki Shimada
Kenjiro Yasuzumi
Soh Futagami
Takashi Tokoro
Manabu Mochizuki

Characteristics of patients with a favorable natural course of myopic choroidal neovascularization

Received: 26 March 2004
Revised: 22 May 2004
Accepted: 27 May 2004
Published online: 28 July 2004

The authors have no financial interest in any products/drugs discussed in this article.

K. Hayashi · K. Ohno-Matsui (✉) · T. Yoshida · K. Kobayashi · A. Kojima · N. Shimada · K. Yasuzumi · S. Futagami · T. Tokoro · M. Mochizuki
Department of Ophthalmology and Visual Science, Graduate School, Tokyo Medical and Dental University, 1-5-45 Yushima, Bunkyo-ku, Tokyo, 113-8519, Japan
e-mail: k.ohno.oph@med.tmd.ac.jp
Tel.: +81-3-58035302
Fax: +81-3-38187188

Abstract *Objective:* To identify the characteristics of patients with myopic choroidal neovascularization (CNV) who had a favorable visual prognosis without treatment. *Methods:* We reviewed the medical records of 52 consecutive patients (57 eyes) with myopic CNV who were followed for at least 5 years after the onset of CNV. Clinical characteristics (patient age, CNV size and location, visual acuity at onset, chorioretinal atrophy development around CNV, and degree of myopia) were compared between patients whose visual acuity 5 years after CNV onset was better than 20/40 and those whose visual acuity was worse than 20/200. *Results:* Among 57 eyes, eight eyes (14.0%; 8 patients) had a final visual acuity better than 20/40. On the other hand, 37 eyes (64.9%; 33 patients) had a final visual acuity worse than 20/200. Statistical analysis revealed that the patients with a good prognosis (final visual acuity better than 20/40) were significantly younger, had significantly smaller CNV, and significantly better initial visual acuity (Mann–Whitney *U*-test, $p<0.05$). Juxtafoveal CNV was more frequently observed in patients with a good prognosis than in those with a poor prognosis (Fisher's exact probability test, $p<0.05$). Only one patient (12.5%) in the good prognosis group developed a very limited area of chorioretinal atrophy around the regressed CNV, while 91.9% of the patients in the poor prognosis group developed chorioretinal atrophy. Refractive status and the axial length measurements did not differ between the two groups. *Conclusions:* Some young patients with myopic CNV retain favorable vision over the long term without active treatment. These information might be useful to predict the visual outcome of patients with myopic CNV.

Introduction

High myopia is a major cause of legal blindness in many developed countries [7, 15, 18]. It affects 27–33% of all myopic eyes, corresponding to a prevalence of 0.2–0.4% in the general population of the United States [15]. High myopia is especially common in Asia and the Middle East [3]. In Japan, pathologic or high myopia affects 6–18% of the myopic population, and around 1% of the general population [17].

Choroidal neovascularization (CNV) is a well-established complication of high myopia. In individuals with an axial length greater than 26.5 mm, 5–10% will develop CNV [14]. High myopia is a frequent cause of CNV in individuals under 50 years of age, accounting for 60% of CNV in a review of young patients in Western Europe [2]. Although the condition is fairly common, the natural history of CNV in high myopia is variable, and most of the reports to date provide conflicting information [1, 9, 10, 16]. In most of the previous studies, the follow-up period was relatively short (no more than a few years) [1, 9, 10, 16]. We recently studied the long-term natural history (>10 years) in a large series of patients with myopic CNV, and reported that in most of the patients with myopic

CNV, visual acuity (VA) decreases to less than 20/200 more than 10 years after the onset. The long-term visual prognosis of myopic CNV is generally poor [22].

The clinical impression is that despite the overall poor prognosis of patients with myopic CNV, some patients retain good vision over the long term without treatment. To avoid unnecessary active treatment of myopic CNV, such as photodynamic therapy or foveal translocation, it is important to identify the characteristics of the patients with myopic CNV whose natural prognosis is favorable. This information might be beneficial for selecting eligible patients for active treatment and excluding patients who might not need active treatment. The present study describes the clinical characteristics of patients with myopic CNV who had a favorable visual outcome without treatment.

Patients and methods

Fifty-two consecutive patients (57 eyes) with high myopia and submacular (subfoveal or juxtafoveal) CNV, identified using clinical records from 1988 to 2002 at the high myopia clinic at the Tokyo Medical and Dental University, were enrolled in the present study. Informed consent was obtained from all patients. The study was approved by the Ethics Committee of the University. Inclusion criteria for this study were (1) refractive error of −8 D or more; (2) fundus changes typical of pathologic myopia: chorioretinal atrophy, lacquer cracks, atrophic patches; (3) presentation within 6 months of onset of symptoms, i.e., loss of VA and/or metamorphopsia; (4) fluorescein angiographic documentation of macular CNV; and (5) minimum follow-up of 5 years. No patients underwent laser photocoagulation, photodynamic therapy or surgical treatment of CNV. Patients with a follow-up of less than 5 years were excluded from the study. Additional exclusion criteria included a history of visual loss due to myopic chorioretinal atrophy or retinal detachment surgery, history of cataract surgery, diabetic retinopathy, or other retinal vascular diseases, age-related maculopathy, dense cataract, glaucoma, and ocular injuries.

The initial evaluation included refraction, axial length measurements, best-corrected visual acuity, detailed fundus drawings using indirect stereoscopic ophthalmoscopy, fluorescein angiography, and color photographs. These procedures were repeated as necessary during the follow-up visits. The early phase of the fluorescein angiogram was independently reviewed by three authors (TY, KOM, and SF), and the size of the CNV on fluorescein angiogram was measured. The case was considered subfoveal if any portion of a new vessel system was below the center of the fovea. Other cases were termed juxtafoveal.

For the purpose of analysis, Snellen visual acuity data were transformed into equivalent logarithms of the minimum angle of resolution (log MAR) values. Data were analyzed using the Mann–Whitney *U*-test, paired *t*-test, or Fisher's exact probability test. A *p*-value of less than 0.05 was considered to be statistically significant.

Results

The patient characteristics are summarized in Table 1. The follow-up period ranged from 60 to 232 months (mean; 107.2±47.6 months). Table 2 gives the number (percentage) of patients who visited at 12, 24, 36, 48, and 60 months after onset of CNV and the mean visual acuity at each follow-up visit. Mean visual acuity (log MAR) is significantly worse at 36, 48, and 60 months compared with initial visual acuity ($p<0.05$, paired *t*-test). Among 57 eyes, eight eyes (14.0%) of eight patients had a final visual acuity better than 20/40. Twelve eyes (21.1%) of 11 patients had a final visual acuity between 20/200 and 20/40. Thirty-seven eyes (64.9%) of 33 patients had a final visual acuity worse than 20/200. In the present study, eight patients whose final visual acuity was better than 20/40 were categorized into the good prognosis group, and 33 patients whose final visual acuity was worse than 20/200 were categorized into the poor prognosis group. Patients and eye characteristics of the good prognosis group are shown in Table 3. Most of these eight patients were relatively young, 20s or 30s, except for two patients (Cases 2 and 8). They also had small CNV, ranging in size from 0.1 DA (disc area) to 0.5 DA except for one patient (Case 6). Half of the patients had juxtafoveal CNV. Only one patient (Case 3) in the good prognosis group developed chorioretinal atrophy around the regressed CNV during the follow-up.

The statistical analysis of the various factors between the good and poor prognosis groups is shown in Table 4. The average age at onset of CNV in the good prognosis group was significantly younger than the average age in poor prognosis group ($p=0.0011$). The average size of CNV in patients in the good visual prognosis group was

Table 1 Patients and study eye characteristics at the initial examination

Gender [persons (eyes)]	
Men	9 (9)
Women	43 (48)
Age (y/o) [mean(SD)]	48.6 (15.0)
Refractive error (*D*) [mean(SD)]	−13.9 (3.7)
Axial length (mm) [mean[SD)]	28.6 (1.6)
The initial Snellen visual avuity (VA)	
>20/40	11/57 (19.3%)
20/40–20/200	34/57 (59.6%)
<20/200	12/57 (21.1%)
Baseline log MAR [mean(SD)]	0.73 (0.49)
Size of CNV (DA) [mean(SD)]	0.85 (0.53)
Location of CNV	
Subfoveal	46/57 (80.7%)
Juxtafoveal	11/57 (19.3%)

CNV choroidal neovascularization, DA disc area

Table 2 Follow-up and visual acuity of the patients

	Number (percentage) of patients	Log MAR	*p*-value
Baseline	57 (100)	0.73	–
12M	54 (94.7)	0.83	n.s.
24M	51 (89.5)	0.89	n.s.
36M	54 (94.7)	0.97	0.01*
48M	57 (100)	1.0	0.001*
60M~	57 (100)	0.96	0.01*

*$p<0.05$, paired *t*-test.

Table 3 Characteristics of the patients with myopic CNV in a good prognosis group

Patient No.	Age	Sex	Refractive error (*D*)	Axial length (mm)	CNV size (disc area)	Location of CNV	Development of chorioretinal atrophy	Initial visual acuity	Final visual acuity	Follow-up period (months)
1	30	F	−10.0	29.3	0.1	J	No	20/30	20/20	77
2	56	F	−11.0	27.7	0.5	J	No	20/200	20/30	70
3	30	M	−13.5	30.5	0.5	S	Yes	20/30	20/30	75
4	24	F	−8.0	28.3	0.3	J	No	20/30	20/30	63
5	26	F	−9.0	27.0	0.3	J	No	20/30	20/20	106
6	29	F	−9.5	28.8	1.5	S	No	20/30	20/20	83
7	32	F	−12.0	31.4	0.2	J	No	20/20	20/20	72
8	48	F	−13.5	29.3	0.5	S	No	20/40	20/30	214

M male, F female, S subfoveal, J juxtafoveal.

Table 4 Comparison of characteristics between groups with good prognosis and poor prognosis

	Good prognosis group (final visual acuity >20/40) (8 eyes)	Poor prognosis group (final visual acuity <20/200) (37 eyes)	*p*-value
Age (y/o)	34.4±11.4	54.0±12.4	0.0011[a]
Refractive error (*D*) [mean(SD)]	10.8±10.9	13.2±3.4	n.s.[a]
Axial length (mm) [mean(SD)]	29.0±1.5	28.1±1.6	n.s.[a]
CNV size (disc area) [mean(SD)]	0.50±0.43	1.01±0.54	0.003[a]
Juxtafoveal CNV	5 eyes (62.5%)	4 eyes (10.1%)	0.0003[b]
Initial visual acuity (log MAR) [mean(SD)]	0.26±0.32	0.93±0.46	0.0002[a]
Chorioretinal atrophy development	1 eye (12.5%)	34 eyes (91.9%)	<0.0001[b]

CNV choroidal neovascularization.
[a] Mann–Whitney *U*-test.
[b] Fisher's exact probability test.

Table 5 Follow-up and visual acuity of the patients in groups with good prognosis and poor prognosis

	Good prognosis group (final visual acuity >20/40) (8 eyes)			Poor prognosis group (final visual acuity <20/200) (37 eyes)		
	Number (percentage) of patients	Log MAR	*p*-value	Number (percentage) of patients	Log MAR	*p*-value
Baseline	8 (100)	0.26	–	37 (100)	0.93	–
12M	8 (100)	0.16	n.s.	35 (94.5)	1.01	n.s.
24M	8 (100)	0.11	n.s.	33 (91.9)	1.11	n.s.
36M	8 (100)	0.11	n.s.	35 (94.6)	1.24	0.003*
48M	8 (100)	0.25	n.s.	37 (100)	1.25	0.001*
60M∼	8 (100)	0.09	n.s.	37 (100)	1.27	0.0003*

*$p<0.05$, paired *t*-test.

significantly smaller than that in the group with poor visual prognosis group ($p=0.003$). Juxtafoveal CNV was more frequently observed in patients in the good visual prognosis group than in those in the poor visual prognosis group ($p=0.0003$). The average log MAR in the good visual prognosis group was significantly better than in the poor visual prognosis group ($p=0.0002$). Thirty-four of 37 eyes (91.9%) in the poor prognosis group developed chorioretinal atrophy around the regressed CNV, while only one patient (Patient 2 in Case report) developed a limited area of chorioretinal atrophy in the good prognosis group ($p<0.01$). On the other hand, there was no statistical difference between refractive status or axial length measurements between the two groups.

Table 5 gives the number (percentage) of patients who visited at 12, 24, 36, 48, and 60 months after onset of CNV and the mean visual acuity at each follow-up visit in the good prognosis group and the poor prognosis group. Mean visual acuity (log MAR) is significantly worse at 36, 48, and 60 months compared with initial visual acuity ($p<0.05$, paired *t*-test) in the poor prognosis group, while visual acuity has not changed significantly at any follow-up visit in the good prognosis group. Representative cases of the good prognosis group are described in the "Case reports."

Case reports

Patient 1

A 24-year-old woman initially presented with decreased vision in her right eye on September 17, 1992. At the initial examination, her best-corrected visual acuity was 20/30 in the right eye and 20/20 in the left. The refractive error was −8.0 D in both eyes, and the axial length measurements were 28.3 mm in the right eye and 27.9 mm in the left. The right fundus at the initial examination had the grayish fibrovascular membrane of CNV (Fig. 1a, arrow) surrounded by subretinal bleeding. Fluorescein fundus angiography after the absorption of bleeding revealed hyperfluorescence at the site of CNV (Fig. 1b, arrow). At the last examination (December 19, 1997), the right fundus had a small regressed CNV (Fig. 1c, arrow), and no bleeding was observed around the CNV. No chorioretinal atrophy was formed around the regressed CNV (Fig. 1c,d). The patient's visual acuity in the right eye remained 20/30 throughout the follow-up.

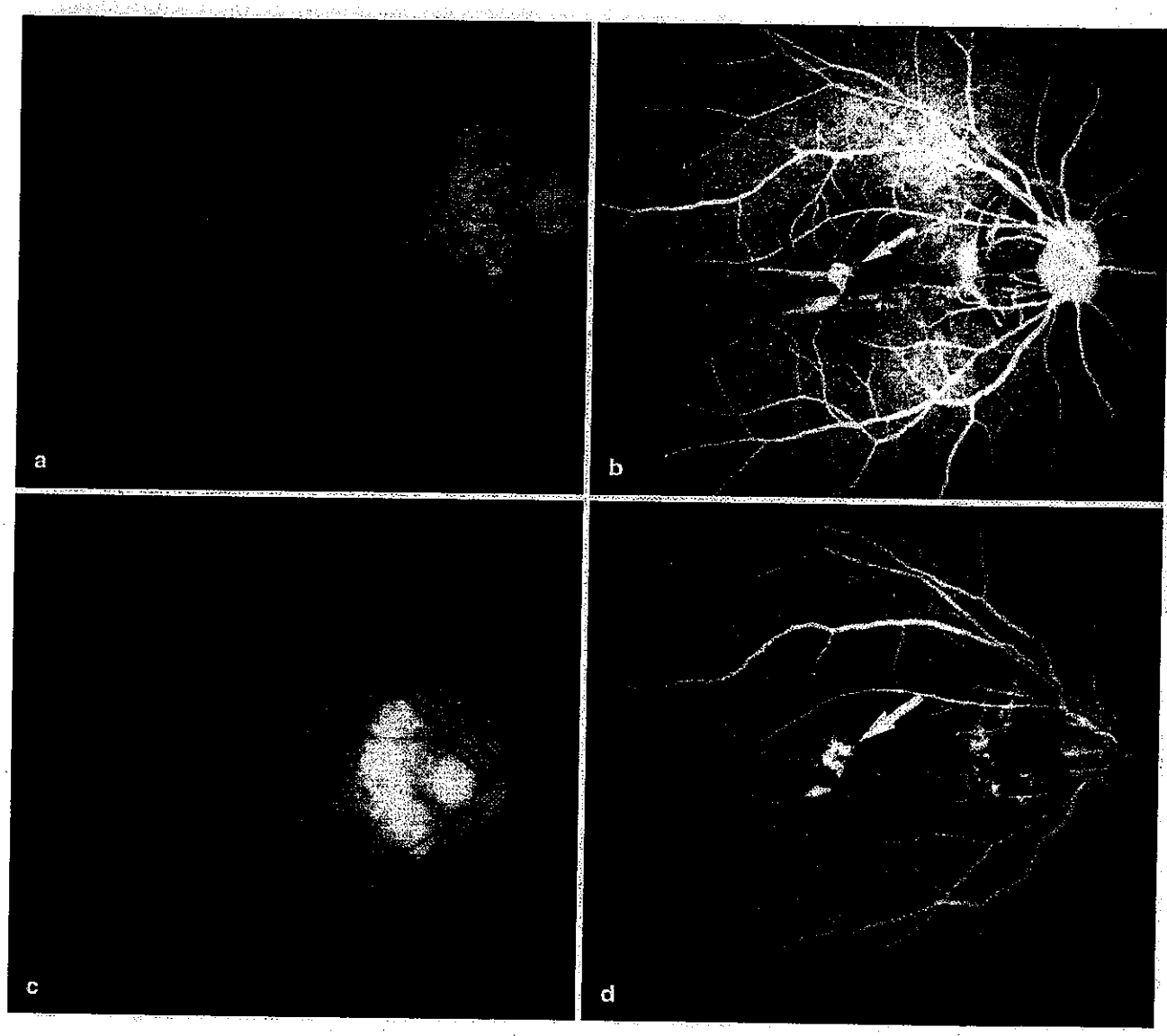

Fig. 1 Patient 1: a 24-year-old woman (Case 4 in Table 2). **a** Right fundus at the initial examination (September 1992) showed a choroidal neovascular membrane (CNV) with bleeding temporal to the macula (*arrow*). Visual acuity was 20/30, and the refractive error was −8.5 D. **b** Fluorescein angiogram at the initial examination. The CNV was hyperfluorescent (*arrow*). Lacquer cracks were observed around the CNV (*arrowhead*). **c** Five years later (December 1997), the CNV regressed and became flat (*arrow*), and no bleeding was observed around the CNV. Chorioretinal atrophy did not develop around the CNV. Visual acuity was 20/30. **d** Fluorescein angiogram at the final examination. The CNV was hyperfluorescent (*arrow*). No chorioretinal atrophy was observed around the CNV

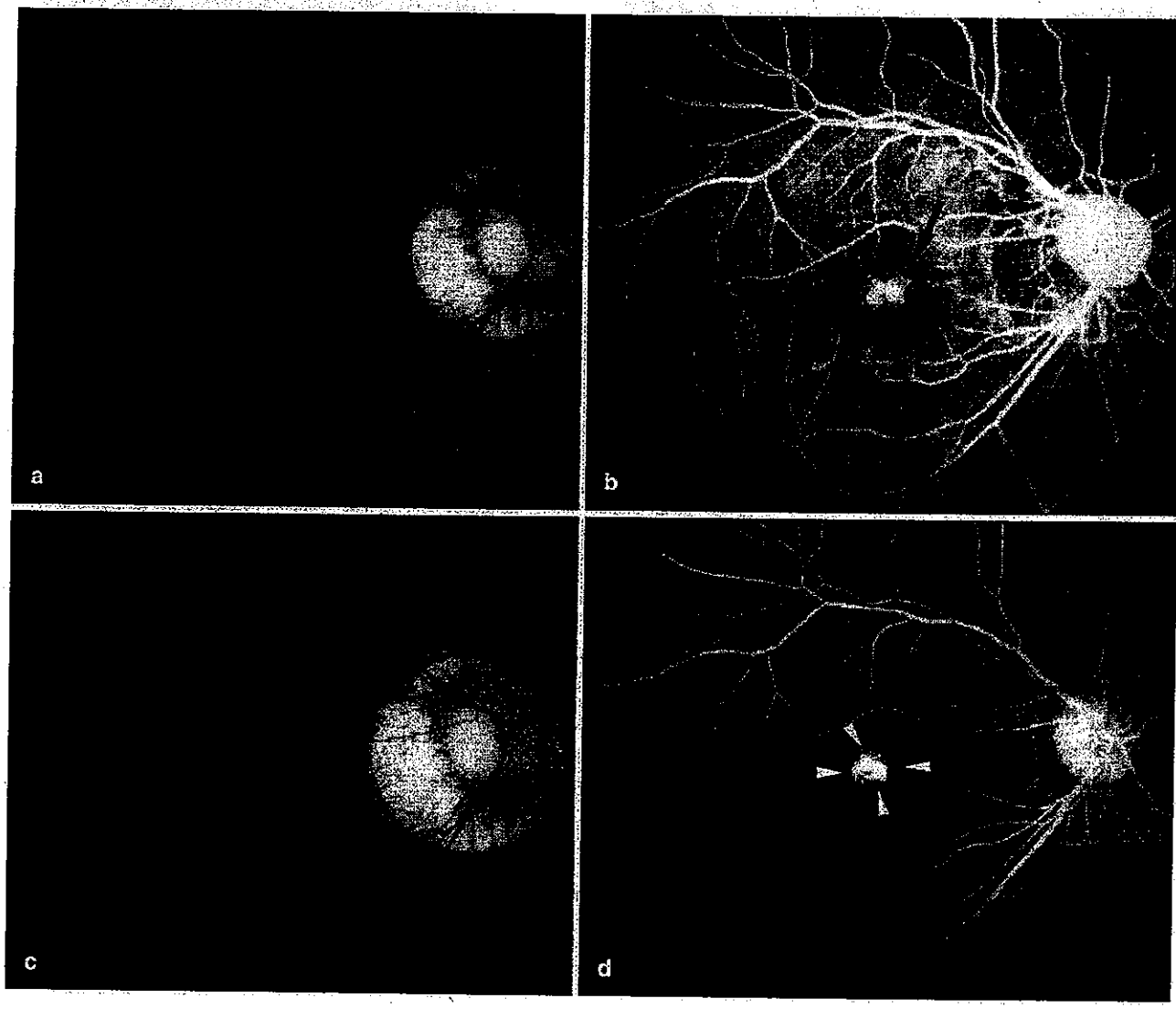

Fig. 2 Patient 2: a 30-year-old man (Case 3 in Table 3). **a** Right fundus at the initial examination (July 1996) showed a choroidal neovascular membrane (CNV) in the macula (*arrow*). Visual acuity was 20/30, and the refractive error was −13.5 D. **b** Fluorescein angiogram at the initial examination. The CNV was hyperfluorescent (*arrow*). Lacquer cracks were observed around the CNV (*arrowhead*). **c** Six years later (October 2002), the CNV regressed and became whitish (*arrow*). Visual acuity was 20/30. **d** Fluorescein angiogram at the final examination. The CNV was hyperfluorescent (*arrow*). A limited area of chorioretinal atrophy was observed around the CNV (*arrowhead*)

Patient 2

A 30-year-old man initially presented with decreased vision in his right eye on July 26, 1996. At the initial examination, his best-corrected visual acuity was 20/30 in the right eye and 20/30 in the left. The refractive error was −13.5 D in the right eye and −13.0 D in the left, and the axial length measurements were 30.5 mm in the right eye and 30.0 mm in the left. The right fundus at the initial examination had the grayish fibrovascular membrane of the CNV (Fig. 2a, arrow). Fluorescein fundus angiography at the initial examination revealed hyperfluorescence at the site of CNV (Fig. 2b, arrow). At the last examination (October 11, 2002), the right fundus had a small regressed CNV (Fig. 2c, arrow), and no bleeding was observed around the CNV. A limited area of chorioretinal atrophy (Fig. 2d, arrowhead) was formed around the regressed CNV (Fig. 2d, arrow). The patient's visual acuity in the right eye remained 20/30 throughout the follow-up.

Discussion

The present study clarified the characteristics of patients with myopic CNV with a favorable natural course. To the best of our knowledge, this is the first report clearly describing the features of patients with myopic CNV who

maintain good vision over the long term without active treatment.

In the present study, eight eyes (14.0%) of eight patients retained a final visual acuity of better than 20/40 over 5 years after the onset of CNV. A statistical analysis of various factors among patients with a good prognosis and those with a poor prognosis revealed several important features. First, the patients with a good prognosis are significantly younger than those with a poor prognosis. This supports our previous findings of a different visual prognosis of myopic CNV among different age groups [21]. Also, the size of CNV of the good prognosis group was significantly smaller than that in the poor prognosis group. Additionally, probably because of the small CNV size, juxtafoveal CNV was more frequently observed in the good prognosis group. Finally, particularly important, only one patient in the good prognosis group developed chorioretinal atrophy around the regressed CNV, while 91.9% of the patients in the poor prognosis group developed chorioretinal atrophy.

Why do the patients with the above characteristics retain good vision over the long term? The development of chorioretinal atrophy around the regressed CNV is a later complication of myopic CNV [3, 19]. We previously reported that the development and enlargement of chorioretinal atrophy around myopic CNV is the most important factor in determining the long-term visual prognosis of myopic CNV [22]. Because myopic CNV has relatively low activity and a self-limiting course, the bleeding from CNV tends to be absorbed rapidly. CNV completely regresses and becomes flat and sometimes unrecognizable over the long term [1, 22]. An area of chorioretinal atrophy develops around myopic CNV, however, and gradually enlarges [19]. Chorioretinal atrophy progresses to involve the fovea centralis, causing eccentric fixation, and resulting in a further decrease in Snellen visual acuity.

In the present study, particularly surprising, only one patient (Case 3 in Table 4) in the good visual prognosis group developed chorioretinal atrophy around the myopic CNV, while 91.9% of the patients in the poor prognosis group developed chorioretinal atrophy. The lack of chorioretinal atrophy is considered to be the deciding factor for a good visual prognosis in patients with myopic CNV.

Although little is known about the mechanism of the development of chorioretinal atrophy around myopic CNV, retinal pigment epithelium (RPE) dysfunction in highly myopic eyes might be involved. Fluorescein fundus angiography sometimes detects a window defect around CNV due to RPE atrophy and the area of the window defect then develops into a typical chorioretinal atrophy (data not shown). RPE function is affected in myopic eyes [8, 11, 20]. Aging is another factor that influences RPE function [4, 5]. Thus, aged patients with high myopia are expected to have more widespread RPE dysfunction than younger patients. In other words, young patients with high myopia might retain relatively better RPE function in general, which might partly explain the lack of chorioretinal atrophy after the regression of CNV in some young myopic patients. This requires further investigation.

Also, in the patients with a good visual prognosis, the size of CNV was smaller than in those with poor prognosis. This supports our previous findings that young patients with myopic CNV had smaller areas of CNV at onset than older subjects [21]. Espinosa-Heidmann et al [6] also reported that age was an independent risk factor for the severity of CNV using an experimentally-induced CNV model. They reported that aged mice demonstrated a much larger CNV area than did young mice. RPE is involved in the induction of CNV as well as in the regression of CNV [12, 13]. Although the mechanism underlying the relation between the size of CNV and patient age is not clear, various degrees of RPE dysfunction among different age groups might be involved in the severity of CNV in addition to the development of chorioretinal atrophy around the CNV.

On the other hand, the degree of myopia (refractive status or axial length measurements) did not differ significantly between patients with a good visual prognosis and those with a poor prognosis. The degree of myopia might not be a major influencing factor for the long-term visual prognosis of myopic CNV.

In summary, we describe the characteristics of patients with myopic CNV with a favorable natural course without any treatments. Thus, it is important to take the above characteristics into consideration to select only eligible patients for active treatment against myopic CNV. The present study suggests that the active treatments like photodynamic therapy should be recommended especially for older subjects with large myopic CNV.

Acknowledgments This work was supported in part by research grant 14571659 from the Japan Society for the Promotion of Science, Tokyo, Japan.

References

1. Avila MP, Weiter JJ, Jalkh AE et al (1984) Natural history of choroidal neovascularization in degenerative myopia. Ophthalmology 91:1573–1581

2. Cohen SY, Laroche A, Leguen Y, Soubrane G, Coscas GJ (1996) Etiology of choroidal neovascularization in young patients. Ophthalmology 103:1241–1244

3. Curtin BJ (1985) Basic science and clinical management. In: Curtin BJ (ed) The Myopias. Harper & Row, Philadelphia, pp 237–245

4. Delori FC, Goger DG, Dorey CK (2001) Age-related accumulation and spatial distribution of lipofuscin in RPE of normal subjects. Invest Ophthalmol Vis Sci 42:1855–1866
5. Docchio F (1989) Ocular fluorometry: principles, fluorophores, instrumentation, and clinical applications. Lasers Surg Med 9:515–532
6. Espinosa-Heidmann DG, Suner I, Hernandez EP et al (2002) Age as an independent risk factor for severity of experimental choroidal neovascularization. Invest Ophthalmol Vis Sci 43:1567–1573
7. Ghafour IM, Allan D, Foulds WS (1983) Common causes of blindness and visual handicap in the West of Scotland. Br J Ophthalmol 67:209–213
8. Harman AM, Hoskins R, Beazley LD (1999) Experimental eye enlargement in mature animals changes the retinal pigment epithelium. Vis Neurosci 16:619–628
9. Hayasaka S, Uchida M, Setogawa T (1990) Subretinal hemorrhages with or without choroidal neovascularization in the maculas of patients with pathologic myopia. Graefes Arch Clin Exp Ophthalmol 228:277–280
10. Hotchkiss ML, Fine SL (1981) Pathologic myopia and choroidal neovascularization. Am J Ophthalmol 91:177–183
11. Kitaya N, Ishiko S, Abiko T et al (2000) Changes in blood–retinal barrier permeability in form deprivation myopia in tree shrews. Vision Res 40:2369–2377
12. Miller H, Miller B, Ryan SJ (1986) The role of retinal pigment epithelium in the involution of subretinal neovascularization. Invest Ophthalmol Vis Sci 27:1644–1652
13. Miller H, Miller B, Ishibashi T, Ryan SJ (1990) Pathogenesis of laser-induced choroidal subretinal neovascularization. Invest Ophthalmol Vis Sci 31:899–908
14. Pruett RC (1994) Pathologic myopia. In: Albert DM and Jakobiec FA (eds) Principles and practice of ophthalmology. Saunders, Philadelphia, pp 878–882
15. Sperduto RD, Seigel D, Roberts J, Rowland M (1983) Prevalence of myopia in the United States. Arch Ophthalmol 101:405–407
16. Tabandeh H, Flynn HW Jr, Scott IU et al (1999) Visual acuity outcomes of patients 50 years of age and older with high myopia and untreated choroidal neovascularization. Ophthalmology 106:2063–2067
17. Tokoro T (1988) On the definition of pathologic myopia in group studies. Acta Ophthalmol 66:107–108
18. Tokoro T (1998) Criteria for diagnosis of pathologic myopia. In: Tokoro T (ed) Atlas of posterior fundus changes in pathologic myopia. Springer, Tokyo, pp 1–2
19. Tokoro T (1998) Myopic choroidal neovascularization (Fuchs' spot). In: Tokoro T (ed) Atlas of posterior fundus changes in pathologic myopia. Springer, New York, Berlin Heidelberg, pp 161–201
20. Yoshida A, Ishiko S, Kojima M (1996) Inward and outward permeability of the blood–retinal barrier in experimental myopia. Graefes Arch Clin Exp Ophthalmol 234:S239–S242
21. Yoshida T, Ohno-Matsui K, Ohtake Y et al (2002) Long-term visual prognosis of choroidal neovascularization in high myopia. A comparison between age groups. Ophthalmology 109:712–719
22. Yoshida T, Ohno-Matsui K, Yasuzumi K et al (2003) Myopic choroidal neovascularization: a 10-year follow-up. Ophthalmology 110:1297–1305

Molecular Vision 2005; 11:1-10 <http://www.molvis.org/molvis/v11/a1>
Received 17 June 2004 | Accepted 7 December 2004 | Published 6 January 2005

The effects of amniotic membrane on retinal pigment epithelial cell differentiation

Kyoko Ohno-Matsui,[1] Shizuko Ichinose,[2] Ken-ichi Nakahama,[3] Takeshi Yoshida,[1] Ariko Kojima,[1] Manabu Mochizuki,[1] Ikuo Morita[3]

[1]Department of Ophthalmology and Visual Science, [2]Instrumental Analysis Research Center, and [3]Section of Cellular Physiological Chemistry, Tokyo Medical and Dental University, Tokyo, Japan

Purpose: To examine the characteristics of retinal pigment epithelial (RPE) cells cultured on amniotic membrane (AM). The present study examined how AM modulates RPE cell differentiation.
Methods: Human RPE cells were cultured on the basement membrane side of dispase treated AM. After one week of cellular confluence, cultures were terminated, conditioned medium was collected, and total RNA was extracted. The expression pattern of several genes considered to participate in the function of differentiated RPE was evaluated. Ultrastructural changes were evaluated by transmission electron microscopy.
Results: Morphologically, RPE cells cultured on AM exhibited ultrastructural epithelial features such as microvilli of the apical membrane and intercellular junctions. Gene expression of RPE65, CRALBP, bestrophin, and tyrosinase related protein (TRP)-2 was upregulated in RPE cells cultured on AM compared to cells cultured on plastic. In addition, protein production of vascular endothelial growth factor, thrombospondin-1, and pigment epithelium derived factor was markedly increased in cells cultivated on AM. Gene expression of cathepsin D, brain derived neurotrophic factor, and basic fibroblast growth factor, however, did not differ between RPE cells cultured on plastic or AM.
Conclusions: RPE cells cultured on AM demonstrated an epithelial phenotype morphologically and several growth factors important for maintaining retinal homeostasis were upregulated. AM might be a useful matrix substrate to retain the differentiated and epithelial phenotype of RPE for subretinal transplantation.

In the western world, age related macular degeneration (AMD) is the primary cause for visual impairment and blindness in individuals over 60 years of age. The most frequent form of AMD (dry AMD) is characterized by primary degeneration and atrophy of the retinal pigment epithelial (RPE) layer. Vision loss in patients with the exudative form of AMD (wet AMD) is caused by the formation of subretinal fibrovascular membranes.

RPE transplantation may be a new treatment strategy for both wet AMD, after removal of the submacular neovascular membrane, and dry AMD. There have been a number of experimental studies on human volunteers in which RPE was grafted into the eyes of patients with advanced AMD [1,2]. The fetal RPE grafts survived for 3 months after subretinal implantation, but there was no evidence of improved function in patients with AMD and subfoveal neovascular membranes [2]. Some of cells transplanted into the subretinal space are randomly organized in multilayers and do not appear to be differentiated [3].

The basement membrane promotes epithelial differentiation [4-6] and prevents epithelial cell apoptosis [7]. It may be that abnormalities of the basement membrane of Bruch's membrane in AMD or after surgical removal of the submacular neovascular membrane can impede the reattachment, survival, proliferation, and biologic function of the transplanted RPE graft. Some studies indicate that RPE does not repopulate as a monolayer over an experimentally damaged Bruch's membrane [8,9].

To preserve cell orientation, some researchers have tried to maintain cell monolayers and polarity using different biologic supports, such as Descemet's membrane [10], the lens capsule [11], Bruch's membrane, blood cryoprecipitates [12], or synthetic supports, such as collagen substrates [13] or biodegradable polymer films [14]. Most of these supports were either toxic to the cells or disintegrated on exposure to liquid media.

The amniotic membrane (AM), with its thick basement membrane and avascular stromal matrix, was recently used as a substrate for the transplantation of cultivated corneal epithelial cells [15]. It is a readily available tissue with many advantages for clinical application. In addition, AM seems to be an immune privileged tissue and contains some immunoregulatory factors, including HLA-G and Fas ligand [16]. We hypothesized that AM might be an ideal matrix substrate to induce and retain the differentiated epithelial phenotype of RPE cells for subretinal transplantation. Proper implantation and orientation of the grafted RPE cells are considered to be important factors for a successful graft because RPE cells are polar with distinct apical/basal characteristics. Implantation of RPE cells cultured on AM might provide a means

Correspondence to: Kyoko Ohno-Matsui, MD, Department of Ophthalmology and Visual Science, Tokyo Medical and Dental University, 1-5-45 Yushima, Bunkyo-ku, Tokyo 113, Japan; Phone: (+81) 3-5803-5302; FAX: (+81) 3-3818-7188; e-mail: k.ohno.oph@tmd.ac.jp

of transplanting an organized sheet of cells for the restoration of normal RPE function over the long term.

As a first step to determine the usefulness of AM as a support matrix for RPE, the present study investigated whether RPE cells can be induced to adopt a differentiated phenotype when grown on AM.

METHODS

Reagents: We obtained Dulbecco's modified Eagle's media (DMEM), and TRIzol reagent from Invitrogen (Carlsbad, CA); plasticware from Falcon and Becton (Dickinson and Co. Franklin Lakes, NJ); fetal calf serum from Hyclone (Logan, UT); vascular endothelial growth factor (VEGF), basic fibroblast growth factor (bFGF), and brain derived neurotrophic factor (BDNF) enzyme linked immunosorbent assay (ELISA) kits, from Genzyme Techne (Minneapolis, MN); You-Prime First-Strand Beads, polymerase chain reaction (PCR) Beads, and Nylon membranes from Amersham Pharmacia Biotech, Inc. (Piscataway, NJ); TSP-1 ELISA kit from Chemicon (Temecula, CA); and agarose from Takara (Ohtsu, Japan).

Culture of human RPE cells: Human RPE cells were kindly supplied by Peter A. Campochiaro, MD (Wilmer Eye Institute, Johns Hopkins University, Baltimore, MD). Human RPE cells were grown in DMEM supplemented with 10% fetal calf serum in a humidified incubator under 95% air and 5% CO_2. Cultures were demonstrated to be pure populations of RPE cells by immunocytochemical staining for cytokeratins (data not shown). Experiments were performed with third or fourth passage cells.

Cultures of RPE on AM: Preserved human AM was purchased from Bio-Tissue (Miami, FL). AM was preserved according to the method described by Lee and Tseng [17]. Briefly, AM derived from cesarean section derived placentas was rinsed in phosphate buffered saline (PBS) containing 100 U/ml penicillin and 0.2 mg/ml streptomycin and stored in a solution of 50% DMEM and 50% glycerol at -80 °C for at least 3 months. After thawing at room temperature, AM was treated with 1.2 U/ml sterile dispase-I solution (Godo-Shusei, Tokyo, Japan) for 30 min and then gently scrubbed with an epithelial scrubber (cell scraper; Costar, Corning, NY), to remove the amni-

Table 1. Primer sequences used for semi-quantitative PCR

Gene	Primer sequence (5'-3') position in mRNA	Annealing temp (°C)	Product size (bp)	Reference
RPE65	F: CCTTTCTTCATGGAGTCTTTG R: ATTGCAGTGGCAGTTGTATTG	52	390	[57]
CRALBP	F: ATGTCAGAAGGGGTGGG R: TCAGAAGGCTGTGTTCTCA	60	953	[57]
TRP2	F: GGAGAAAAGTACGACAGAGACAAGG R: AGAAAAGCCAACAGCACAAAAAGAC	60	1542	[25]
tyrosinase	F: GCATCATTCTTCTCCTCTTGG R: ATAGGATCGTTGGCAGATCC	60	359	[25]
cathepsin D	F: GTGCTTCACAGTCGTCTTC R: GAGCCATAGTGGATGTCAAAC	55	172	[58]
bFGF	F: GCCTTCCCGCCCGGCCACTTCAAGG R: GCACACACTCCTTTGATAGACACAA	55	179	[57]
BDNF	F: ATGACCATCCTTTTCCTTACTATGGT R: TCTTCCCCTTTTAATGGTCAATGTAC	52	741	[57]
PEDF	F: GGACGCTGGATTAGAAGGCAG R: TTGTATGCATTGAAACCTTACAGG	64	675	[39]
FGFR	F: GGGTCCATCAATCACACGTAC R: GGCGTGTTGTTATCCTCACCAG	60	643	[21]
bestrophin	F: GGCCAGATCTATGTACTGGAATAAGCCCGAGC R: GGCCCTCGAGTTAGGAATGTGCTTCATCCCTG	65	773	[36]
β-actin	F: GAGCACAGAGCCTCGCCTTTGC R: GGATCTTCATGAGGTAGTCAGTCAGG	65	620	[57]

This table describes the primer sequences used in RT-PCR. The results of RT-PCR are shown in Figure 4.

otic epithelium without breaking the underlying basement membrane. The AM was sutured onto a culture insert (Millicell-CM, Millipore, Bedford, MA) with a non-absorbable suture with the basement membrane facing up and placed in a 6 well tissue culture plastic plate, as described by Meller and Tseng [18]. RPE cells were seeded at a density of $1.0x10^5$ cells/culture insert on the AM. The cultures were incubated at 37 °C in 5% CO_2 and 95% air, and the medium was changed every 2 days.

In some experiments, RPE cells were cultured on uncoated plastic in DMEM with 10% FBS and used as controls. Each condition was prepared in triplicate, and experiments were performed at least three times with reproducible results.

F-actin immunostaining of RPE cells on AM: RPE monolayers were washed three times with PBS, fixed with 1.0% paraformaldehyde in PBS for 10 min, permeabilized with 0.1% Triton X-100 for 5 min in PBS, washed in PBS, stained with FITC conjugated phalloidin for 40 min then washed two times in PBS. The distribution of F-actin was visualized and de-

Table 2. Primer sequences used for real-time quantitative PCR

Gene	Primer sequence (5'-3') position in mRNA	Annealing temp (°C)	Product size (bp)	Accession number
RPE65	F: CCTTTCTTCATGGAGTCTTTG R: ATTGCAGTGGCAGTTGTATTG	50	122	BC075035
CRALBP	F: GCTGCTGGAGAATGAGGAAACT R: TGAACCGGGCTGGGAAGGAATC	61	149	BC004199
TRP2	F: GGTTCCTTTCTTTCCAGT R: GAAGAAAAGCCAACAGCACAA	60	185	S69231
bestrophin	F: ATGGGGCCTTGATGGSAGCAC R: GGCGAAGCATCCCCATTAGG	58	227	BC015220
GAPDH	F: TGAACGGAAGCTCACTGG R: TCCACCACCCTGTTGCTGTA	65	307	M33197

Some of the primers listed in Table 1 were used for the detection of tyrosinase, cathepsin D, bFGF, BDNF, PEDF, and FGFR.

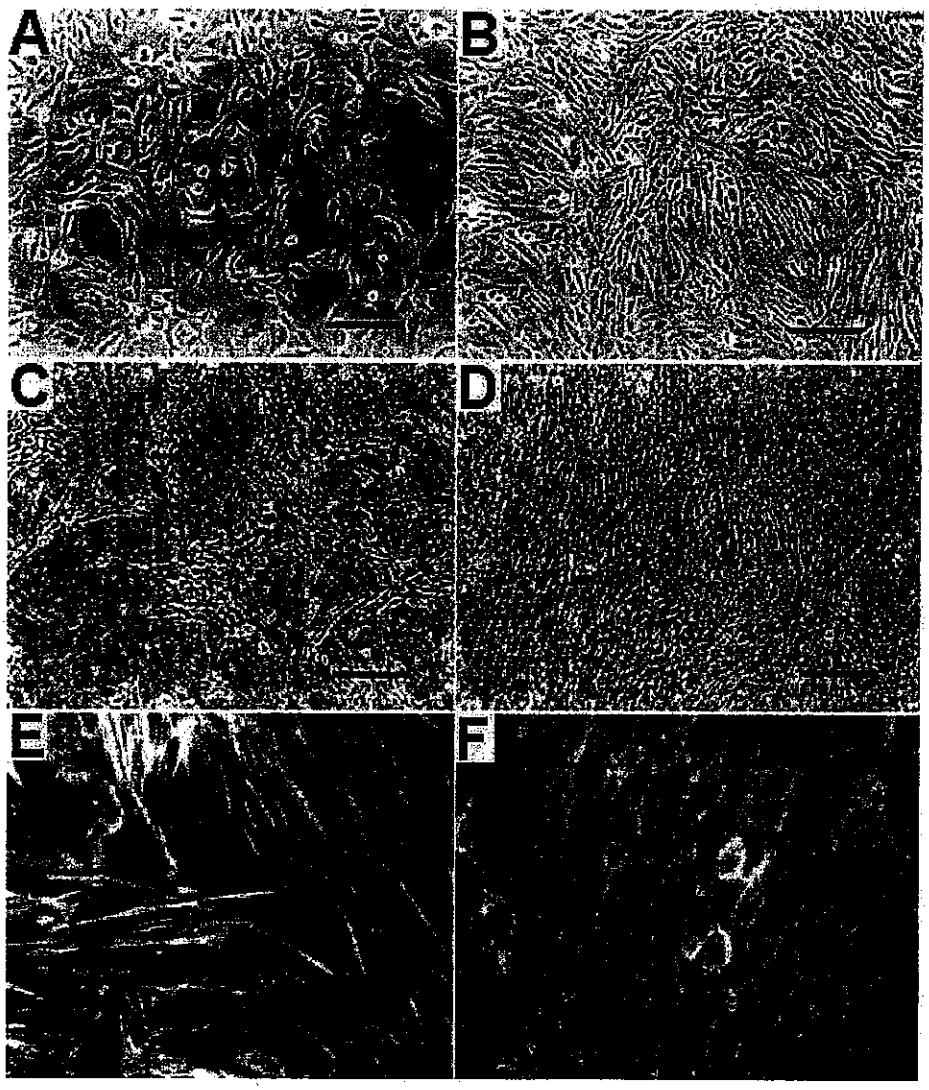

Figure 1. Phase contrast micrographs and F-actin immunostaining. Human RPE cells cultured on plastic one day after seeding (**A**) and at confluence (**B**). Human RPE cells cultured on amniotic membrane (AM) one day after seeding (**C**) and at confluence (**D**). F-actin immunostaining in confluent RPE cells on plastic (**E**) and on AM (**F**). Scale bars in **A-D** represent 100 µm; scale bars in **E** and **F** represent 15 µm.

tected under a fluorescence microscope.

Electron microscopy: RPE cell cultures on denuded AM were examined by transmission electron microscopy. On day 14, cultures on denuded AM were fixed in 2.5% glutaraldehyde in 0.1 M PBS for 2 h. The cultures were washed overnight at 4 °C in the same buffer and post-fixed with aqueous osmium tetroxide with 0.1 M PBS for 2 h. The pellets were dehydrated through a graded ethanol series, and embedded in Epon 812. Semi-thin (1 µm) sections for light microscopy were collected on glass slides and stained for 30 s with toluidine blue; ultrathin (70 nm) sections were collected on copper grids and double stained with uranyl acetate and lead citrate and then examined with an H-7100 transmission electron microscope (Hitachi Ltd., Hitachinaka, Japan).

Semiquantitative reverse transcription-PCR: Total RNA was extracted from RPE cells using TRIzol reagent. cDNA was synthesized from 2 µg of total RNA using You-Prime First-Strand Beads according to the manufacturer's protocol, and reaction product was submitted to PCR amplification using GeneAmp PCR System (Perkin-Elmer Cetus Corp., Norwalk, CT). The expression of mRNA for the discriminative cellular markers RPE 65, cellular retinaldehyde binding protein (CRALBP), and bestrophin was examined. The growth factors and trophic factors investigated were pigment epithelium derived factor (PEDF), BDNF, and bFGF. Also, the enzymes involved in melanin synthesis, tyrosinase and tyrosinase related protein (TRP)-2, were examined. A special lysosomal enzyme in RPE cells, cathepsin D, was also examined [19]. The expression of FGFR2, an isoform of the FGF receptor that is upregulated as a function of differentiation in RPE cells [20], was also examined. Oligonucleotide primers complimentary to the 5' and 3' ends were used in the RT-PCR studies (Table 1). PCR products (8 µl) were electrophoresed with a 2% agarose gel that contained 0.5% ethidium bromide, and specific DNA bands were examined under an ultraviolet transilluminator.

Real-time PCR: To confirm mRNA expression and to evaluate the mRNA expression levels in the cultured cells, real-time PCR was applied using specific primers (Table 2) with a Light Cycler™ instrument (Roche Diagnostics, Basel, Switzerland). Some primers were redesigned to produce a product of size between 100 bp to 200 bp. Each 25 µl of PCR

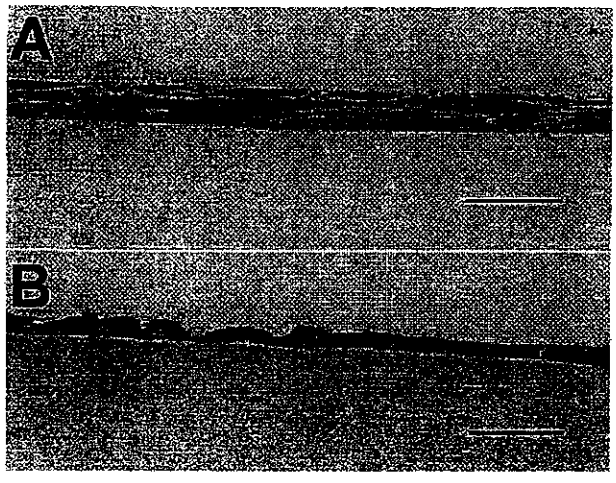

Figure 2. Different morphology of RPE cells cultured on plastic and on amniotic membrane. Toluidine blue stained sections of RPE cells on plastic (**A**) and RPE cells after 14 days cultivation on amniotic membrane (**B**). Scale bars represent 50 µm.

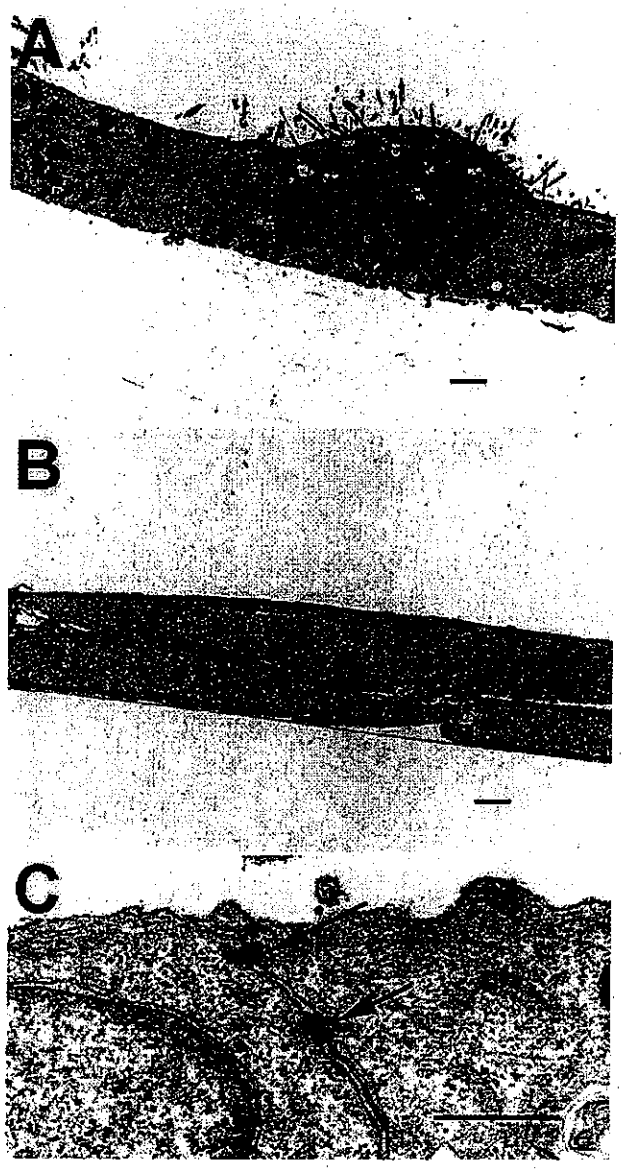

Figure 3. Transmission electron micrographs of cultivated RPE cells on denuded amniotic membrane for two weeks. **A**: Electron micrographs show a tight monolayer of cuboidal to spheroidal RPE cells growing over amoniotic membrane (AM). A heterogenous expression of apical microvilli was observed on the apical side. **B**: RPE cells cultured on plastic show elongated cell shape in multilayers. **C**: Electron micrographs reveal junctional specializations on the apical side between adjacent cells cultured on AM. Scale bars represent 1 µm.

mixture contained 0.3 μM of gene specific primers, 1 μl of sample cDNA solution, 12.5 μl of PCR mixture (Quantitect SYBR Green PCR Kit™ Qiagen Inc., CA) and 6.5 μl of supplied water. PCR was performed with the first cycle at 95 °C for 15 min to activate HotStar Taq polymerase in the premixture, this was followed by 45 cycles of 94 °C for 30 s, 55 °C for 30 s, and 72 °C for 30 s. The signal intensity was measured at 72 °C during each cycle. The absence of bands other than the target band was verified by gel electrophoresis on 1.5% agarose stained with ethidium bromide under UV light after amplifications. The original PCR product containing 25 ng/μl of target DNA was diluted into concentrations of 10^{-4}, 10^{-5}, 10^{-6}, 10^{-7}, 10^{-8}, 10^{-9}, and 10^{-10} with distilled water, and these dilutions were simultaneously subjected to real-time PCR to establish a standard curve. To adjust the difference of concentration of mRNA reverse transcribed, GAPDH was used as an internal control. Relative quantity was evaluated by ratio of mRNA expression of the target gene and GAPDH.

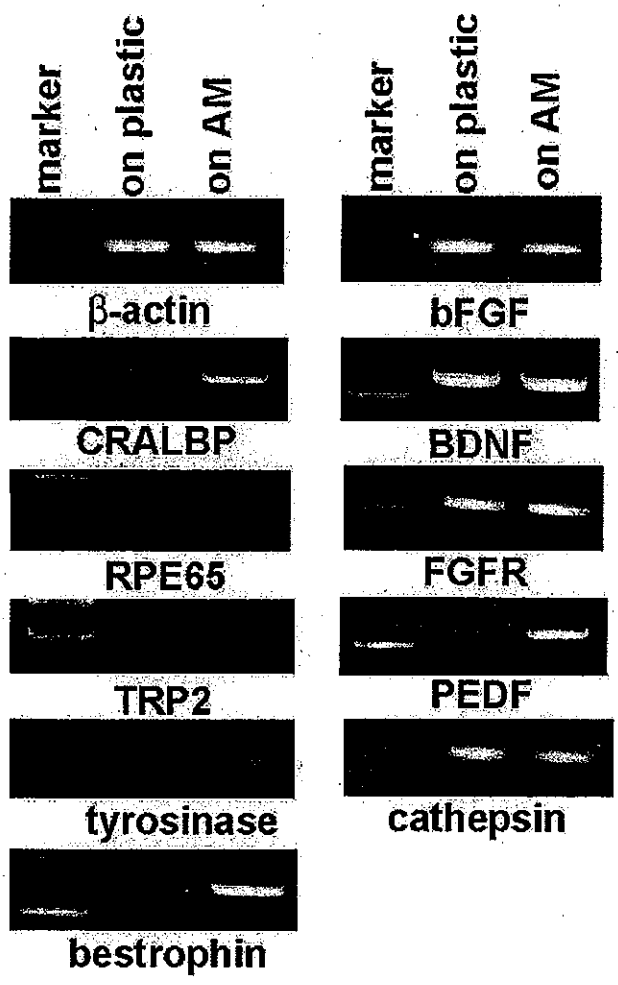

Figure 4. RT-PCR analysis of discriminatory molecules and growth and trophic factors in RPE cells. Total RNA was extracted from confluent RPE cells cultured on either plastic or amniotic membrane (AM). RT-PCR was performed on 2 μg RNA. For each gel shown, the left lane (labeled "marker") is a commercially supplied size marker, the middle lane (labeled "on plastic") is product from a reaction using RNA from RPE cells cultured on plastic, and the right lane (labeled "on AM") is a product from a reaction using RNA from RPE cells cultured on AM. cDNA product (2 μl) from RT-PCRs that used β-actin primers was used for all PCR reactions and β-actin was used as a positive control throughout.

ELISA of growth factors: Cells were incubated in serum free medium for 48 h before harvest for protein concentration. The amount of secreted VEGF, BDNF, and bFGF in RPE conditioned culture medium was determined using commercial ELISA kits (Genzyme Techne), according to the manufacturer's instructions. Also, the amount of secreted thrombospondin (TSP)-1 was determined using a commercial ELISA kit (Chemicon, Temecula, CA). The lowest detection limit of each molecule by ELISA assay was as follows: VEGF, 5 pg/ml; BDNF, 20 pg/ml; bFGF, 7 pg/ml; and TSP-1, 3.91 ng/ml. After the conditioned medium was collected, cells were washed with PBS, detached from the dish by treatment with 0.2% trypsin-EDTA, and suspended in 1 ml PBS. The number of viable cells was determined using a Coulter Counter Channelyzer (Coulter Electronics, Krefeld, Germany).

Western blot analysis of PEDF: Cells were allowed to condition serum free medium for 48 h before harvest for protein concentration. Final protein concentrations were determined using the BCA assay (Pierce Chemical Co., Rockford, IL) according to the manufacturer's instructions. Equal amounts of secreted protein (8 μg) were separated by 12% sodium dodecyl sulfate-polyacrylamide gel electrophoresis and transblotted onto nylon membranes. Nylon membranes containing transblotted proteins were pretreated with 1.0% nonfat dried milk in 50 mM Tris buffer (pH 8.0), followed by incubation overnight with a monoclonal antibody against human PEDF (dilution 1:4000, Transgenic Co., Kumamoto, Japan). PEDF immunoreactivity was visualized by exposing X-ray film to blots incubated with the ECL reagent.

Table 3. Results of real-time PCR

Gene	AM to plastic ratio
RPE	12.80
CRALBP	5.00
TRP2	12.30
tyrosinase	0.89
cathepsin D	0.78
bFGF	0.52
BDNF	1.02
PEDF	8.22
FGFR	1.11
bestrophin	13.50

The fold changes in mRNA levels of the selected genes were determined by real-time RT-PCR. Values represent fold changes of mRNA levels of RPE cells on amniotic membrane compared to RPE cells on plastic (AM to plastic ratio) after normalization for GAPDH content. Data are means of 3 to 4 samples per group.

RESULTS

Morphology of RPE cell cultures on AM: The human RPE cells cultured over dispase treated AM fragments were attached to the epithelial basement membrane side within 24 h of seeding. After settling down, RPE cells displayed many connected colonies comprised of small, polygonal, and uniform epithelial cells (Figure 1C). Three days after seeding, RPE cells cultured on plastic or AM reached confluence (Figure 1B,D). F-actin staining using FITC-phalloidin demonstrated the formation of actin stress fibers and altered cell shape to fusiform pattern in RPE cells cultured on plastic (Figure 1E). In contrast, the actin staining in RPE cells cultivated on AM revealed actin fibers arranged in a radial and circumferential pattern (Figure 1F). When RPE cells were seeded over AM, semithin sections stained with toluidine blue demonstrated that the cells were organized in a tight monolayer of round cells (Figure 2B). In contrast, RPE cells cultivated on plastic showed fusiform and elongated cells in multilayers (Figure 2A). Electron micrographs showed a tight monolayer of spheroidal RPE cells growing over AM (Figure 3A), different from elongated RPE cells in multilayers when cultured on plastic (Figure 3B). Ultrastructurally, RPE cells cultured on AM contained well developed cell organelles, including mitochondria, endoplasmic reticula, and Golgi apparatuses, and large quantities of free ribosomes. Electron micrographs revealed junctional specializations on the apical side between adjacent cells (Figure 3C) and showed a heterogenous expression of apical microvilli (Figure 3A).

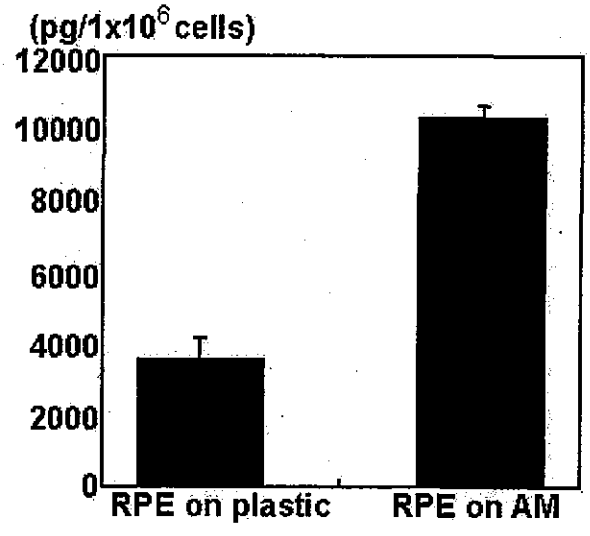

Figure 5. Increased secretion of VEGF in RPE cells cultured on amniotic membrane. Concentration of immunoreactive VEGF in supernatants of RPE cells cultured on either plastic or amniotic membrane. Cells were incubated in serum free medium for 48 h before harvest for protein concentration, and the amount of secreted VEGF in RPE conditioned culture medium was determined using commercial ELISA kits. The data show that VEGF secretion is increased in RPE cells cultured on amniotic membrane compared to cells on plastic ($p<0.01$).

Reverse transcription PCR: The discriminatory molecule RPE 65, an RPE specific molecule that is thought to have an important role in the RPE-photoreceptor vitamin A cycle, CRALBP, which is involved in the regeneration of visual pigment, and bestrophin, which is a late marker of RPE differentiation [21], were all detected by RT-PCR in RPE cells cultured on plastic and on AM (Figure 4). Expression levels of RPE 65, CRALBP, and bestrophin were significantly increased in RPE cells cultured on AM compared to cells cultured on plastic. According to the results of real-time PCR, the ratio of RPE 65/GAPDH, CRALBP/GAPDH, and bestrophin/GAPDH of cells cultured on AM compared to that of cells on plastic was 12.8, 5.0, and 13.5 times, respectively (Table 3). On the other hand, there was no apparent difference in mRNA expression of cathepsin D, a major photoreceptor outer segment digestive protease in the retina [22-24], between RPE cells cultured on either plastic or AM.

The expression of a panel of growth and trophic factors with the potential to affect both RPE and photoreceptor cell function and survival were also investigated by RT-PCR. Positive mRNA expression was observed for BDNF, bFGF, and PEDF (Figure 4). The expression of PEDF mRNA was markedly elevated in RPE cells cultured on AM compared to those cultured on plastic, while there was no apparent difference in the mRNA expression of bFGF and BDNF (Figure 4). According to the results of real-time PCR, the ratio of PEDF/GAPDH in cells on AM compared to that in cells on plastic was 8.2 times (Table 3). The expression and alternative splicing of FGF receptors is regulated by cellular differentiation in vitro [20]. mRNA expression of FGFR2 was detected both in RPE cells cultured on plastic those cultured on AM, but there was no apparent difference (Figure 4).

Tyrosinase and TRP-2 are the enzymes involved in melanin biosynthesis, and are expressed in melanocytes of neural crest origin and RPE cells [25,26]. There was no apparent difference in the expression of mRNA of tyrosinase, however, TRP-2 mRNA expression was markedly upregulated when cells were cultivated on AM (Figure 4). According to the results of real-time PCR, the ratio of TRP-2/GAPDH in cells on AM compared to that in cells on plastic was 12.3 times (Table 3).

Secretion of growth and trophic factors: ELISAs were performed on serial dilutions of RPE cell culture supernatants, conditioned for 2 days, from a minimum of three independent experiments. VEGF was positively detected in RPE cells cultured on plastic or AM. Secretion of VEGF in RPE cells cultured on AM was more than three fold higher than in RPE cells cultured on plastic ($p<0.01$, Figure 5). Also, the secretion of TSP-1 in RPE cells cultured on AM was approximately three fold higher than in RPE cells on plastic ($p<0.01$, Figure 6). On the other hand, BDNF and bFGF were not detected above the limit of the assays both in conditioned medium from RPE cells on plastic or on AM (data not shown).

Western blotting of PEDF: Western blot analysis using monoclonal antibody against purified PEDF protein (Transgenic, Inc., Kumamoto, Japan) was performed. PEDF antibody recognized a 50 kDa protein species in medium con-

ditioned by RPE cells cultured on AM (Figure 7). PEDF protein was not detected in the conditioned medium from RPE cells cultured on plastic or of AM only.

DISCUSSION

Although RPE cell transplantation remains a potentially useful approach for the treatment of AMD and other retinal diseases like retinitis pigmentosa, prolonged improvement of the vision of patients that received RPE cell suspension transplantations into the subretinal space has not been obtained. The main disadvantage of cell suspension transplantation is the random organization in multilayers of transplanted cells in the subretinal space of the host [3].

The human AM is a thin and elastic tissue that forms the inner layer of the amniotic sac. Human AM, with its thick basement membrane and avascular stromal matrix, has been successfully used for surface reconstruction in a variety of ocular surface disorders [27]. In the present study, we hypothesized that AM might be a feasible support substrate for transplanted RPE cells because AM can be obtained more easily than any other nonsynthetic carrier such as Descemet's membrane, and it has been used for cultured corneal epithelial cell transplantation with good clinical results [28,29]. AM was reported to induce non-goblet epithelial differentiation in cultured rabbit conjunctival epithelial cells [18]. Implantation of AM into the rabbit subretinal space is feasible and well tolerated by the rabbit retina [30].

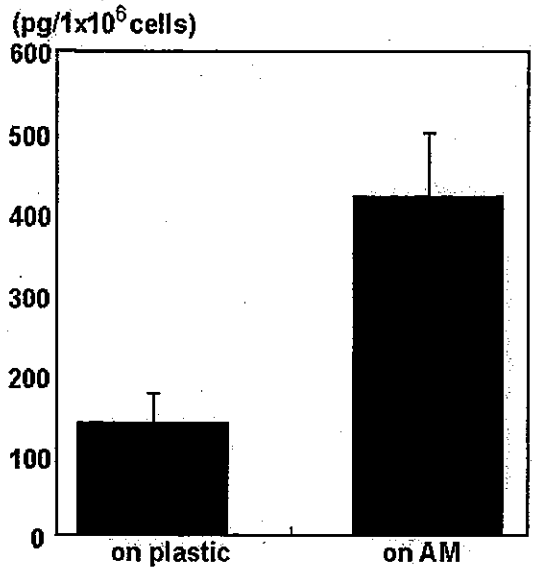

Figure 6. Increased secretion of thrombospondin-1 in RPE cells cultured on amniotic membrane. Concentration of immunoreactive thrombospondin-1 in supernatants of RPE cells cultured on either plastic or amniotic membrane. Cells were incubated in serum free medium for 48 h before harvest for protein concentration, and the amount of secreted thrombospondin-1 in RPE-conditioned culture medium was determined using commercial ELISA kits. The data show that thrombospondin-1 secretion is increased in RPE cells cultured on amniotic membrane compared to cells on plastic ($p<0.01$).

As a first step to evaluate the usefulness of AM as a support for transplanted RPE cells, we investigated the characteristics of RPE cells cultured on human AM. After seeding, human RPE cells spread easily and constituted tight colonies on AM. Using transmission electron microscopy, we identified a monolayer of RPE cells in which integration with the substrate and cell-cell contacts were detected, as reported by Capeans et al. [31]. We also observed that RPE cells cultured on AM exhibited ultrastructural epithelial features such as microvilli of the apical membrane and intercellular junctions, similar to RPE cells in situ.

We then investigated the expression pattern of several genes considered to participate in the function of differentiated RPE. Alge et al. [32] performed comparative proteome analysis of native differentiated and cultured dedifferentiated human RPE cells, and reported that RPE 65 and CRALBP were present only in native differentiated cells. Alizadeh et al. [33], using Northern blot analysis, also demonstrated that in ARPE-19 cells, a spontaneously differentiated RPE cell line, mRNA expression of CRALBP and RPE 65 was upregulated. Bestrophin is the protein altered in Best vitelliform macular dystrophy [34], an inherited retinal degenerative disease similar to AMD. Bestrophin is considered a very late marker of RPE differentiation during normal development [21], and bestrophin localizes to the basolateral plasma membrane of the RPE, which suggests that bestrophin contributes to the transepithelial potential of RPE [35]. In the present study, the mRNA expression of RPE 65, CRALBP, and bestrophin was clearly upregulated in RPE cells cultured on AM compared to cells cultured on plastic, which suggests that AM facilitates RPE expression of differentiated features [32,33]. On the other hand, we did not detect any difference in mRNA expression of cathepsin D between RPE cells cultured on plastic or on AM. Cathepsin D is a major digestive protease of photoreceptor outer segments in the retina [22]. Alge et al. [32] also reported that the expression pattern of proteins involved in phagocytosis and exocytosis, including cathepsin D, was not different between native RPE and dedifferentiated cultured RPE cells using comparative proteome analysis, which indicates that cathepsin D expression might not be influenced by the differentiation status of RPE cells.

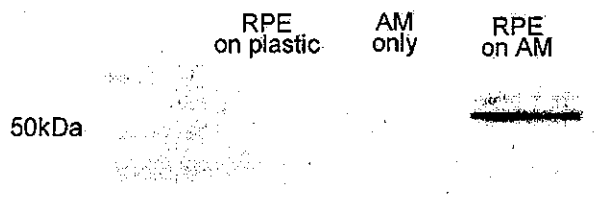

Figure 7. Representative western analysis of PEDF protein. The lanes from left to right are a commercially supplied size marker (unlabeled); proteins in medium conditioned for two days by RPE cells cultured on plastic (labeled "RPE on plastic"); proteins in medium conditioned for 2 days by amniotic membrane (AM) only, without seeding RPE cells on it (labeled "AM only"); and proteins in medium conditioned for two days by RPE cells on AM (labeled "RPE on AM").

The RPE is located between the neural retina and the vascular choroid and influences the structure and function of the cells in both, mediated mainly by secretion of various growth factors. In the present study, we focused on the expression of BDNF, bFGF, VEGF, PEDF, and TSP-1 from RPE cells among various factors secreted from RPE. Hackett et al. [36] showed that ARPE-19 has a high level of BDNF mRNA. Although mRNA expression of BDNF and bFGF was noted both in RPE cells cultured on plastic or AM in our study, we did not detect either protein in the RPE cell supernatant using ELISA. In addition, mRNA expression of FGFR-2, an FGF receptor that is upregulated by differentiation of ARPE-19 cells [20], was not different between cells cultured on plastic or on AM.

VEGF and PEDF expression was dramatically increased in RPE cells cultivated on AM. VEGF protein secretion was three times higher in the medium conditioned by RPE cells cultured on AM compared to that conditioned by RPE cells cultured on plastic. In addition, PEDF production was markedly increased when RPE cells were cultured on AM. The PEDF protein signal was completely absent in RPE cells cultured on plastic by western blotting; however, PEDF secretion dramatically increased in RPE cells cultured on AM. PEDF is a 50 kDa protein initially purified from the conditioned medium of human fetal RPE cells as a factor that induces neuronal differentiation of cultured Y79 retinoblastoma cells [37]. The gene is also called early population doubling level cDNA-1 [38]. PEDF is the most potent natural inhibitor of angiogenesis, and is a key factor associated with avascularity of the cornea, vitreous, and outer retinal layer of the eye [39]. Semokava et al. [40] also demonstrated that PEDF has a key role in retinal homeostasis by subretinal transplantation of genetically modified PEDF expressing iris pigment epithelial cells. We previously demonstrated a marked increase of VEGF and PEDF expression in differentiated RPE cells cultured on laminin, and suggested that a balance between high levels of both VEGF and PEDF might be important to maintain the homeostasis of the human retina [41]. Based on our previous studies [41,42], we speculated that in normal healthy conditions, the RPE has a positive survival effect on the maintenance of the highly vascularized, highly permeable fenestrated choriocapillaris on its outer basal aspect by secreting VEGF, while maintaining the complete avascularity of the photoreceptor layer internal to the RPE by secreting PEDF. Thus, expression of high levels of both VEGF and PEDF might be a property of the differentiated RPE.

TSP-1 protein secretion is also markedly increased in RPE cells cultured on AM. TSP-1 is a cell attachment factor with cell specific activity and the most prevalent TSP molecule found in vivo [43,44]. TSP-1 profoundly inhibits angiogenesis, both in vivo and in vitro [45-47]. Miyajima-Uchida et al. [47] reported that human RPE cells produce TSP-1, TSP-1 accumulates in the cytoplasm of RPE cells in vivo and in vitro, and suggested that TSP-1 is an important control factor in choroidal neovascularization. Considering these findings, increased production of TSP-1 by RPE cells cultured on AM might prevent the development of choroidal neovascularization and maintain the avascularity of the outer retina, together with PEDF.

Tyrosinase and TRP are enzymes involved in melanin synthesis. In particular, TRP-2 is an early differentiation marker for melanoblasts and RPE [48]. Although we did not detect any difference in mRNA expression of tyrosinase, TRP2 expression was markedly upregulated in RPE cells cultured on AM. Fang et al. [49] demonstrated that treatment of human cutaneous melanocytes with the differentiation inducer hexamethylene bisacetamide (HMBA) dramatically increased the expression of TRP-2 without changing the morphology, and suggested that the TRP-2 gene can be selectively modulated in melanocyte differentiation. TRP-2 might also have a role in the modulation of apoptotic pathways in melanoma cells [50]. Thus, accumulation of TRP-2 in RPE cells cultured on AM might protect transplanted cells from apoptosis.

Future studies are needed to determine which components of AM are responsible for controlling the phenotypic alterations of RPE. Growth factors contained in AM might have a role. Koizumi et al. [51] reported that AM preserved at -80 °C expressed the proteins of several growth factors (EGF, TGF-a, KGF, HGF, bFGF, TGF-b_1, TGF-b_2, TGF-b_3). AM without amniotic epithelium, however, had significantly lower levels of these growth factors, suggesting that the growth factors have an epithelial origin. In the present study, we removed the epithelium from AM before seeding the RPE. Neither BDNF nor bFGF protein, which induce differentiation in RPE cells [36,52,53], was detected in the supernatants of RPE cells cultured on AM. It is unlikely that these growth factors actively participate in phenotypic alteration of RPE cells cultured on AM.

Besides soluble factors, the extracellular matrix might have an important role in differentiation of epithelial cells. Immunohistochemical study revealed the presence of collagen (types 1, 3, 4, and 5) and fibronectin throughout the whole AM and the expression of collagen 7 and laminin-5 on the basement membrane side of AM [54]. A matrix component, laminin-5, has a crucial role in the proliferation, differentiation, and migration of corneal epithelial cells [55]. Laminin-5 might be one candidate for an important component in AM to induce phenotypic alteration in RPE cells.

In conclusion, this study demonstrated that AM induces phenotypic alterations in RPE cells. The epithelial phenotype is observed morphologically and upregulation of several growth factors important for maintaining retinal homeostasis occurs. This suggests that an RPE cell sheet cultivated on AM can be transplanted. By transplanting the RPE cell sheet maintaining the epithelial phenotype on AM, RPE cells on AM retain a monolayer and epithelial, differentiated phenotype in the subretinal space of the host for a long term. Simultaneously increased expression of a panel of genes necessary to maintain retinal homeostasis, as shown in the present study, might be needed for transplanted RPE cells. The use of AM as a basement membrane support might be expanded to other cell sources. Iris pigment epithelial cells, which have the same embryonic origin as RPE cells, are a possible candidate. More-

over, in regenerative medicine, there is a potential for embryonic stem cells [56] for use in clinical treatments. A combination of these cells with a basement membrane support like AM might be more advantageous for subretinal transplantation in the future.

ACKNOWLEDGEMENTS

The authors thank Peter A. Campochiaro and Sean F. Hackett for human RPE cells. The authors thank Tomoko Yoshida for her excellent technical support and Yoshio Miki for gene analysis.

REFERENCES

1. Peyman GA, Blinder KJ, Paris CL, Alturki W, Nelson NC Jr, Desai U. A technique for retinal pigment epithelium transplantation for age-related macular degeneration secondary to extensive subfoveal scarring. Ophthalmic Surg 1991; 22:102-8.
2. Algvere PV, Berglin L, Gouras P, Sheng Y, Kopp ED. Transplantation of RPE in age-related macular degeneration: observations in disciform lesions and dry RPE atrophy. Graefes Arch Clin Exp Ophthalmol 1997; 235:149-58.
3. Crafoord S, Algvere PV, Seregard S, Kopp ED. Long-term outcome of RPE allografts to the subretinal space of rabbits. Acta Ophthalmol Scand 1999; 77:247-54.
4. Guo M, Grinnell F. Basement membrane and human epidermal differentiation in vitro. J Invest Dermatol 1989; 93:372-8.
5. Streuli CH, Bailey N, Bissell MJ. Control of mammary epithelial differentiation: basement membrane induces tissue-specific gene expression in the absence of cell-cell interaction and morphological polarity. J Cell Biol 1991; 115:1383-95.
6. Kurpakus MA, Stock EL, Jones JC. The role of the basement membrane in differential expression of keratin proteins in epithelial cells. Dev Biol 1992; 150:243-55.
7. Boudreau N, Sympson CJ, Werb Z, Bissell MJ. Suppression of ICE and apoptosis in mammary epithelial cells by extracellular matrix. Science 1995; 267:891-3.
8. Shiragami C, Matsuo T, Shiraga F, Matsuo N. Transplanted and repopulated retinal pigment epithelial cells on damaged Bruch's membrane in rabbits. Br J Ophthalmol 1998; 82:1056-62.
9. Tezel TH, Kaplan HJ, Del Priore LV. Fate of human retinal pigment epithelial cells seeded onto layers of human Bruch's membrane. Invest Ophthalmol Vis Sci 1999; 40:467-76.
10. Thumann G, Schraermeyer U, Bartz-Schmidt KU, Heimann K. Descemet's membrane as membranous support in RPE/IPE transplantation. Curr Eye Res 1997; 16:1236-8.
11. Hartmann U, Sistani F, Steinhorst UH. Human and porcine anterior lens capsule as support for growing and grafting retinal pigment epithelium and iris pigment epithelium. Graefes Arch Clin Exp Ophthalmol 1999; 237:940-5.
12. Farrokh-Siar L, Rezai KA, Patel SC, Ernest JT. Cryoprecipitate: An autologous substrate for human fetal retinal pigment epithelium. Curr Eye Res 1999; 19:89-94.
13. Bhatt NS, Newsome DA, Fenech T, Hessburg TP, Diamond JG, Miceli MV, Kratz KE, Oliver PD. Experimental transplantation of human retinal pigment epithelial cells on collagen substrates. Am J Ophthalmol 1994; 117:214-21.
14. Lu L, Garcia CA, Mikos AG. Retinal pigment epithelium cell culture on thin biodegradable poly(DL-lactic-co-glycolic acid) films. J Biomater Sci Polym Ed 1998; 9:1187-205.
15. Koizumi N, Fullwood NJ, Bairaktaris G, Inatomi T, Kinoshita S, Quantock AJ. Cultivation of corneal epithelial cells on intact and denuded human amniotic membrane. Invest Ophthalmol Vis Sci 2000; 41:2506-13.
16. Kubo M, Sonoda Y, Muramatsu R, Usui M. Immunogenicity of human amniotic membrane in experimental xenotransplantation. Invest Ophthalmol Vis Sci 2001; 42:1539-46.
17. Lee SH, Tseng SC. Amniotic membrane transplantation for persistent epithelial defects with ulceration. Am J Ophthalmol 1997; 123:303-12.
18. Meller D, Tseng SC. Conjunctival epithelial cell differentiation on amniotic membrane. Invest Ophthalmol Vis Sci 1999; 40:878-86.
19. Sugano E, Tomita H, Abe T, Yamashita A, Tamai M. Comparative study of cathepsins D and S in rat IPE and RPE cells. Exp Eye Res 2003; 77:203-9.
20. Alizadeh M, Miyamura N, Handa JT, Hjelmeland LM. Human RPE cells express the FGFR2IIIc and FGFR3IIIc splice variants and FGF9 as a potential high affinity ligand. Exp Eye Res 2003; 76:249-56.
21. Bakall B, Marmorstein LY, Hoppe G, Peachey NS, Wadelius C, Marmorstein AD. Expression and localization of bestrophin during normal mouse development. Invest Ophthalmol Vis Sci 2003; 44:3622-8.
22. Rakoczy PE, Mann K, Cavaney DM, Robertson T, Papadimitreou J, Constable IJ. Detection and possible functions of a cysteine protease involved in digestion of rod outer segments by retinal pigment epithelial cells. Invest Ophthalmol Vis Sci 1994; 35:4100-8.
23. Wilcox DK. Vectorial accumulation of cathepsin D in retinal pigmented epithelium: effects of age. Invest Ophthalmol Vis Sci 1988; 29:1205-12.
24. Udono T, Takahashi K, Yasumoto K, Yoshizawa M, Takeda K, Abe T, Tamai M, Shibahara S. Expression of tyrosinase-related protein 2/DOPAchrome tautomerase in the retinoblastoma. Exp Eye Res 2001; 72:225-34.
25. Abul-Hassan K, Walmsley R, Tombran-Tink J, Boulton M. Regulation of tyrosinase expression and activity in cultured human retinal pigment epithelial cells. Pigment Cell Res 2000; 13:436-41.
26. Smith SB, Zhou BK, Orlow SJ. Expression of tyrosinase and the tyrosinase related proteins in the Mitfvit (vitiligo) mouse eye: implications for the function of the microphthalmia transcription factor. Exp Eye Res 1998; 66:403-10.
27. Tseng SC, Prabhasawat P, Lee SH. Amniotic membrane transplantation for conjunctival surface reconstruction. Am J Ophthalmol 1997; 124:765-74.
28. Koizumi N, Inatomi T, Suzuki T, Sotozono C, Kinoshita S. Cultivated corneal epithelial stem cell transplantation in ocular surface disorders. Ophthalmology 2001; 108:1569-74.
29. Shimazaki J, Aiba M, Goto E, Kato N, Shimmura S, Tsubota K. Transplantation of human limbal epithelium cultivated on amniotic membrane for the treatment of severe ocular surface disorders. Ophthalmology 2002; 109:1285-90.
30. Rosenfeld PJ, Merritt J, Hernandez E, Meller D, Rosa RH Jr, Tseng SCG. Subretinal implantation of human amniotic membrane: a rabbit model for the replacement of Bruch's membrane during submacular surgery. Invest Ophthalmol Vis Sci 1999; 40:S206.
31. Capeans C, Pineiro A, Pardo M, Sueiro-Lopez C, Blanco MJ, Dominguez F, Sanchez-Salorio M. Amniotic membrane as support for human retinal pigment epithelium (RPE) cell growth. Acta Ophthalmol Scand 2003; 81:271-7.
32. Alge CS, Suppmann S, Priglinger SG, Neubauer AS, May CA, Hauck S, Welge-Lussen U, Ueffing M, Kampik A. Compara-